Desalination and Water Treatment
www.deswater.com
doi: 10.1080/19443994.2014.968907

55 (2015) 3247–3252
September

Taylor & Francis
Taylor & Francis Group

Numerical investigation on characteristics of falling film in horizontal-tube falling film evaporator

Qing-gang Qiu, Wei-guo Jiang, Sheng-qiang Shen*, Xiao-jing Zhu, Xing-sen Mu

School of Energy and Power Engineering, Dalian University of Technology, Dalian 116024, China,
email: zzbsheng@dlut.edu.cn (S.-q. Shen)

Received 31 March 2014; Accepted 16 June 2014

ABSTRACT

Horizontal-tube falling film technology is widely used in multi-effect desalination plant. The film characteristics of falling water film outside the tubes in horizontal-tube falling film evaporator were simulated. The numerical result was compared with the experimental result and they were proven with good agreement. The film thickness distribution at different Reynolds number and different circular angle had been investigated. Also, the effects of liquid flow rate and tube diameter on the film thickness distribution were discussed in detail. Numerical simulation result shows that, with the increase in Reynolds number, the falling film thickness at a certain circumferential angle increases with almost linear growth rate, and the thinnest film at the surface of the tube appears at the angle of about 120°. The result also indicates that the local dry out spot on the surface of the tube would occur when the fluid flow rate decreases to a certain value. In addition, the film thickness decreases with the increase in the tube diameter at a fixed fluid flow rate.

Keywords: Falling film thickness; Falling film distribution; Horizontal-tube falling film evaporator

1. Introduction

Falling liquid film outside the surface of a horizontal tube is an important and commonly used heat transfer process in heat exchangers, especially in the multi-effect evaporation desalination plant. Horizontal-tube falling film evaporator has lot of advantages compared with other evaporation technology, such as higher heat transfer coefficient, smaller liquid flow rate, smaller temperature difference, and simple structure. It also offers advantage in dealing with liquid distribution, non-condensable gases, fouling, and many other operating problems of the heat exchangers [1–3]. As a kind of energy-saving technology, the lower grade waste heat can be used and the heat consumption of the technology is considerably small. Due to all these advantages, many scholars around the world have been attracted and done extensive researches [4–10]. However, most of these studies focused on heat transfer performance of tubes using experimental or theoretical methods and few of them considered the film thickness and film distribution outside the tubes.

*Corresponding author.

Presented at the Conference on Desalination for the Environment: Clean Water and Energy
11–15 May 2014, Limassol, Cyprus

During the process of falling liquid flow outside horizontal tubes, the heat and mass transfer processes are coupled with each other, and the falling liquid is the main carrier of heat transferred from horizontal tube. The flow uniformity is usually considered as the key factor for the horizontal-tube falling film evaporator to operate regularly [11–13]. Both inadequate liquid supply and overfeeding liquid are adverse and very likely causes a series of problems, such as fouling, corrosion, and drastic reduction in heat transfer performance. Thus, it is extremely significant to study the film distribution along the tubes and explore corresponding mechanism. In this paper, the numerical simulation is presented to study the film thickness distribution on the horizontal tube surface and the effects of liquid flow rate, tube diameter, and position angle along tube are discussed in detail.

2. Numerical model and method

A two-dimensional physical model which consists of two staggered tubes is built in this paper. It is assumed that the falling film throughout the solution domain is viscous, laminar flow. The flow process is adiabatic and happens under the normal conditions of which the ambient temperature is 25℃ and the pressure is 101.325 kPa. The working medium within computational domain is liquid–gas two-phase flow.

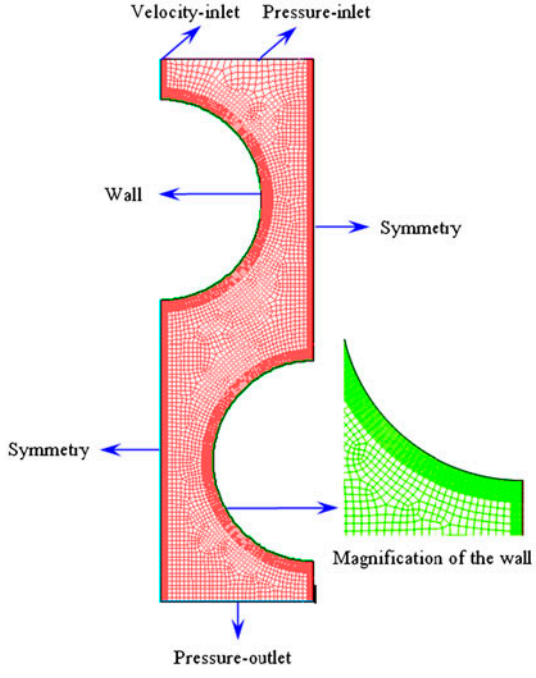

Fig. 1. Numerical model of horizontal tube with the boundary conditions.

The distilled water is chosen as the liquid phase and the air is chosen as the gas phase.

The computational domain is discretized by quadrilateral mesh, as shown in Fig. 1. The solution domain is discretized by quadrilateral elements. A boundary layer technique for the region near the tube wall and very fine meshes for the region with two-phase flow are used to precisely capture the mass transfer process around the horizontal tube. A very small region on the left of solution domain top is set as the velocity inlet and this region represent the liquid flow path to the top of the tube. The rest of the top is set as the pressure inlet. The whole bottom of the solution domain is set as pressure outlet with specified constant pressure. The tube wall is supposed to be a no-slip, smooth wall. The calculated region is initially set to be fully filled with air, and the volume fraction of liquid water at the velocity inlet is set as 1. In addition, a wall contact angle, which is used to adjust the surface normal in the cells near the wall, is specified as 0° to ensure the complete wetting of the wall in the simulation.

The mass conservation can be derived by applying Reynolds transport theorem to any material volume in the computational domain. The mass within a material volume is constant for incompressible fluid and thus the derivative of the mass with respect to time equals to zero:

$$\mathrm{div}(\mathbf{U}) = 0 \tag{1}$$

The momentum conservation is given as:

$$\frac{\partial(u)}{\partial t} + \mathrm{div}(u\mathbf{U}) = \mathrm{div}(\upsilon \mathrm{grad} u) - \frac{1}{\rho}\frac{\partial p}{\partial x} + S_u \tag{2}$$

and:

$$\frac{\partial(v)}{\partial t} + \mathrm{div}(v\mathbf{U}) = \mathrm{div}(\upsilon \mathrm{grad} v) - \frac{1}{\rho}\frac{\partial p}{\partial y} + S_v \tag{3}$$

where S_u and S_v are the general source terms, equal to zero for the incompressible fluid with constant viscosity.

The finite volume method is employed here to translate these coupled [14–17], partial differential equations into algebraic expressions that can be solved using a computer. In this process, the motion and continuity equations are integrated for each computational cell and then discretized with the second-order upwind scheme. The discretized equations are linearized and solved in a segregated, first-order implicit manner. The

pressure-implicit with splitting of operators method is used to relate the solution of the continuity equation to the pressure correction. The volume of fluid method is used as multi-phase flow model to capture the free surface of gas–liquid two-phase flow. In present study, the gas phase, air, is defined as the principle phase of which the volume fraction is represented by α_1 while the liquid phase, water, is defined as the second phase of which the volume fraction is represented by α_2. The continuity equation can be slightly modified to be solved for the second phase, water:

$$\frac{\partial \alpha_2}{\partial t} + \vec{u} \cdot \nabla \alpha_2 = 0 \tag{4}$$

and the solution for the volume fraction for principle phase, air, is given as:

$$\alpha_1 = 1 - \alpha_2 \tag{5}$$

Based on Eqs. (6) and (7), it can be seen that a mesh cell is entirely filled with liquid for $\alpha_2 = 1$, with gas for $\alpha_2 = 0$, and with gas–liquid two phase for $0 < \alpha_2 < 1$. The properties of two-phase flow in each cell can thus be obtained in the form of weighted average values:

$$\rho = \alpha_2 \rho_2 + (1 - \alpha_2)\rho_1 \tag{6}$$

$$\mu = \alpha_2 \mu_2 + (1 - \alpha_2)\mu_1 \tag{7}$$

where ρ and μ are the evaluated density and viscosity within the cell, ρ_1, ρ_2 and μ_1, μ_2 are the densities and viscosities of phase 1 and phase 2, respectively.

3. Results and discussion

Numerical simulation is presented to reveal the effects of liquid flow rate and tube diameter size on the film thickness and film distribution in different cases. Although the cases involved in this study are all in steady state, the liquid film waves are in a very small scale during the calculation process. Therefore, the measured film thickness, which is exactly captured when the water volume fraction is 0.5, is actually the time-averaged value at a certain point in a period of time.

3.1. Validation of the numerical model and method

The simulation results of falling film thickness at Reynolds number of 574 and tube spacing of 6.4, 9.5, and 19.4 mm are showed in Fig. 2. All data are measured at the circumferential angle of 180°. To verify the simulation results, all these data are compared with the experimental results by Gstoehl [18] and the theoretical results by Nusselt [13] which are all shown in Fig. 2. From Fig. 2, it can be found out that the simulated results agree well with the experimental results when Re is 574, and the average film thickness decreases with the increase in tube spacing. The reason is that with the increase in distributor height, the flow rate of liquid film at the moment that liquid just impacts the tube surface becomes larger and the initial formation of liquid droplet becomes more unstable. Therefore, the droplet spraying on the film has more influence on film flow rate. This phenomenon also verifies the inversely proportional relationship between the thickness of liquid film and the liquid flow rate. It should be noticed that although the film thickness distributions around the tube wall agree well with the experimental results under the same condition, it has certain deviation with Nusselt's theoretical results when the circumferential angle is greater than 90°. The film thickness around the tube wall first decreases, and then increases after it reaches the minimum value. This variation trend apparently conforms to the Nusselt's parabola theory. However, in the circumferential range greater than 90° the film thickness increase slowly with the increase in circumferential angle. The possible reason is that the flow in this region, from 90° to 180°, is the fully developed laminar flow, and the thin liquid film forms well. The volume force dominates liquid surface tension forces and volume flow tends to be stable, and this is the reason that the simulation results doesn't agree well with

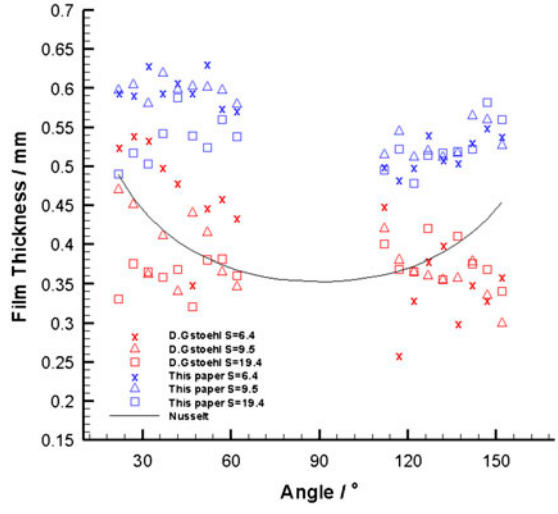

Fig. 2. Film thickness vs. angle while Re = 574.

Nusselt's theoretical results. In addition, it also can be seen that the liquid film waves in the region between 20° and 45° becomes steady in the range from 45° to 90°. This simulation results agree well with Roger's theory which is about the developing zone and fully developed zone. In present study, the circumferential region from 0° to 45°can be considered as the developing zone of falling film, in which the film thickness produces slight waves. While the rest of tube surface can be considered as the fully developed zone in which the film thickness decreases smoothly.

3.2. Effect of flow rate on the falling film distribution

The flow rate is a parameter that not only determines the flow behavior along the tube surface, but also it is closely related to the occurrence of so called "dry zone" on the surface of the tube. Fig. 3 illustrates the film thickness distribution at different flow rates. It can be seen that the film thickness increases with the increase in flow rate. For a certain flow rate, e.g. 0.3 kg/ms, the film thickness decreases from the top region of the tube and then increases gradually. When the flow rate is less than 0.1 kg/ms, the wall surface can only be covered with a layer of very thin liquid film, which shows a trend of droplet flow mode. If the flow rate continues to decrease, the liquid film cannot be fully formed and the local dry zone on the tube surface occurs. To avoid the occurrence of dry zone on the tube surface in practical case, the flow rate of liquid film should be kept greater than a certain value.

3.3. Influence of tube diameter on the falling film distribution

The diameter of tube is an important structure parameter that relates to the heat transfer efficiency and manufacture cost of a falling film horizontal-tube evaporator.

Fig. 4 show the effects of tube diameter on film thickness with different flow rates. The tube diameter, D, widely varies from 19 to 120 mm. The film thickness is measured at the circumferential position of 90° on the tube surface. The curves in Fig. 4 illustrate that the film thickness decreases with the increase in diameter size and increases with an increase in flow rate. When the flow rate is less than a certain value, e.g. 0.1 kg/ms, the film thickness on the tube surface is very thin and the liquid film may not be successfully generated all over the tube surface and under this circumstances, the dry zone is formed.

3.4. Effect of Reynolds number on the falling film thickness

Fig. 5 shows the film thickness variations at the circumferential angles of 45° and 135° on the tube surface with Reynolds number from 100 to 1,000 and tube spacing, S, from 6 to 19.

As can be seen from Fig. 5, the liquid film thickness at the certain angle of the tube increases with increasing Reynolds number and the growth rate is approximately linear. When the angle is 45°, liquid film thickness increases with an increase in tube spacing and the curve of variation trend is smooth. The reason may be that the flow of liquid film is in the fully developed zone and the flow is in stable state. When the circumferential angle is 135°, the film flow is unstable and the liquid film largely fluctuates. Therefore, the thinnest film of falling film flow on the horizontal tube should appear around the circumferential angle of 135°.

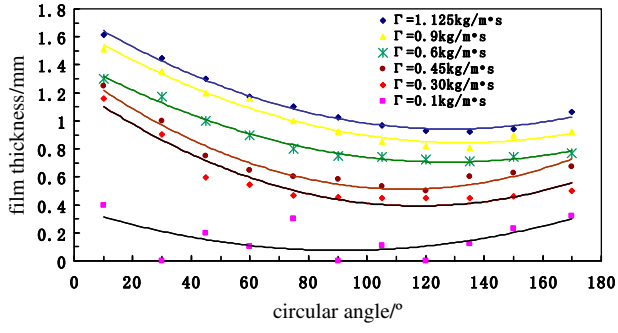

Fig. 3. Distribution curve of film thickness with different flow rates.

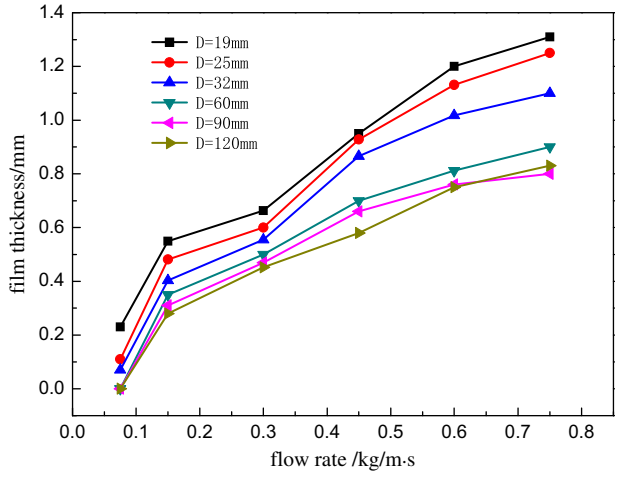

Fig. 4. Effect of tube diameter on film thickness with different flow rates.

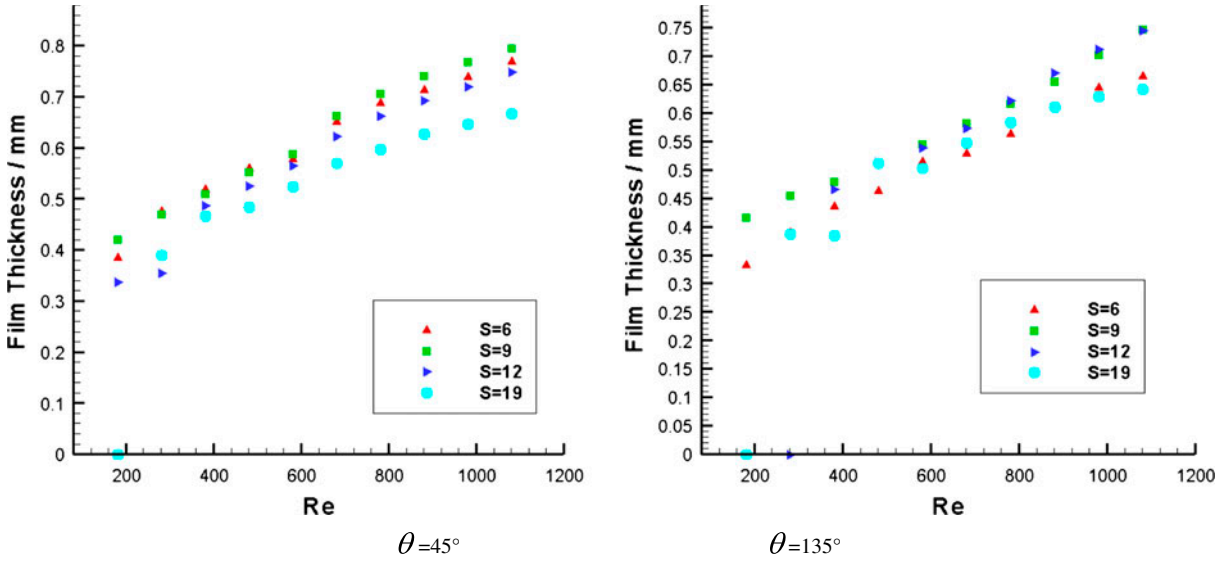

Fig. 5. Film thickness vs. Re while $\theta = 45^{\circ}$ and $\theta = 135^{\circ}$.

4. Conclusions

Numerical simulation was performed to study the film thickness and distribution outside the tubes in horizontal-tube falling film evaporator. Several aspects that have influence on the of film thickness were investigated, such as the flow rate, the diameter, and Reynolds number. Comparisons between the numerical result and the experimental result were performed and analyzed. The effects of different factors should be considered in designing the horizontal-tube falling film evaporator. Global optimization should be performed for better design of the evaporator structure. The results may provide a basis and guidance for further research on the characteristics of falling film flows, which could also offer necessary support for heat and mass transfer. Conclusions obtained so far are summarized below:

(1) The film thickness decreases from the top of the tube first and then increases around the perimeter of the tube after a minimum value around the circumferential 120° position angle is reached. Liquid accumulates together at the bottom of the tube due to the combined influence of gravity and surface tension.
(2) The film thickness decreases with the reduction of flow rate at a certain circumferential position. When the flow rate is less than a certain value, the liquid film cannot be successfully formed and the local dry zone on the tube surface may occur and this phenomena should be avoided from happening in practical cases.
(3) The film thickness decreases with the increase in diameter size at a certain circumferential position. It waves sharply along the tube when the diameter size is small. With the increase in diameter size, the liquid film distribution is more uniform.
(4) With the increase in Reynolds number, the falling film fluctuates and the film thickness at a certain circumferential angle increases, and the growth rate is approximately linear.

Acknowledgments

This project was supported by National Natural Science Foundation of China (51336001). The authors are grateful for this support.

References

[1] Y. Fujita, M. Tsutsui, Experimental investigation of falling film evaporation on horizontal tubes, Heat Transfer-Jpn. Res. 27(8) (1998) 609–618.
[2] A.M.I. Mohamed, Flow behavior of liquid falling film on a horizontal rotating tube, Exp. Therm. Fluid Sci. 31 (2007) 325–332.
[3] G. Ribatski, A.M. Jacobi, Falling-film evaporation on horizontal tubes—A critical review, Int. J. Refrig. 28 (2005) 635–653.
[4] A. Solan, A. Zfati, Heat transfer in laminar flow of a liquid film on a horizontal cylinder, Proceedings of the Fifth International Heat Transfer Conference, 1974, Paper FC 2.9, Tokyo.

[5] L. Yang, S. Shen, Experimental study of falling film evaporation heat transfer outside horizontal tubes, Desalination 220 (2008) 654–660.
[6] R. Armbruster, J. Mitrovic, Evaporative cooling of a falling water film on horizontal tubes, Exp. Therm. Fluid Sci. 18 (1998) 183–194.
[7] J.T. Rogers, S.S. Goindi, Experimental laminar falling film heat transfer coefficients on a large diameter horizontal tube, Can. J. Chem. Eng. 67 (1989) 560–568.
[8] J. Mitrovie, Influence of tube spacing and flow rate on heat transfer from a horizontal tube to a falling liquid film, in: Proceedings of the Eighth International Heat Transfer Conference, 1986, vol. 4, pp. 1949–1956, San Francisco, CA.
[9] Y. Fujita, M. Tsutsui, Evaporation heat transfer of falling films on horizontal tube. Part 2. Experimental study, Heat Transfer-Jpn. Res. 24 (1995) 17–31.
[10] R. Armbruster, J. Mitrovic, Heat transfer in falling film on a horizontal tube, in: Proceedings of 1995 National Heat Transfer Conference—vol. 12, ASME HTD 314 (1995) 13–21.
[11] M.C. Chyu, A.E. Bergles, An analytical and experimental study of falling-film evaporation on a horizontal tube, J. Heat Transfer 109 (1987) 983–990.
[12] V. Slesarenko, Hydrodynamics and heat exchange during film evaporation of sea water in a vapourwater up flow, Desalination 33 (1980) 251–257.
[13] W. Nusselt, Die oberflachenkondensation des wasserdampfes. Zeitschrift des Vereines Deutscher Ingenieure (Surface condensation of water vapor. Association of German Engineers) (1916) 541–546, 569–575.
[14] C.W. Hirt, B.D. Nichols, Volume of fluid (VOF) method for the dynamics of free boundaries, J. Comput. Phys. 39 (1981) 201–225.
[15] D. de Niem, E Kührt, U. Motschmann, A volume-of-fluid method for simulation of compressible axisymmetric multi-material flow, Comput. Phys. Commun. 176 (2007) 170–190.
[16] K.M.T. Kleefsman, A Volume-of-Fluid based simulation method for wave impact problems, J. Comput. Phys. 206 (2005) 363–393.
[17] C.W. Hirt, B.D. Nichols, Volume of fluid (VOF) method for the dynamics of free boundaries, J. Comput. Phys. 39 (1981) 201–225.
[18] D. Gstoehl, J.F. Roques, P. Crisinel, J.R. Thome, Measurement of falling film thickness around a horizontal tube using a laser Measurement Technique, Heat Transfer Eng. 25(8) (2004) 28–34.